

# 2016 SNMMI Highlights Lecture: Neurosciences

Alexander Drzezga, MD, University Hospital of Cologne, Germany

*From the Newsline Editor: The Highlights Lecture, presented at the closing session of each SNMMI Annual Meeting, was originated and presented for more than 33 years by Henry N. Wagner, Jr., MD. Beginning in 2010, the duties of summarizing selected significant presentations at the meeting were divided annually among 4 distinguished nuclear and molecular medicine subject matter experts. Each year Newsline publishes these lectures and selected images. The 2016 Highlights Lectures were delivered on June 15 at the SNMMI Annual Meeting in San Diego, CA. In this issue we feature the lecture by Alexander Drzezga, MD, Professor and Chair in Nuclear Medicine at the University Hospital of Cologne (Germany), who spoke on highlights in the neurosciences. Note that in the following presentation summary, numerals in brackets represent abstract numbers as published in The Journal of Nuclear Medicine (2016;57 [suppl 2]).*

**T**he task of summarizing the neuroscience highlights from this year's SNMMI Annual Meeting is challenging. Many interesting and significant studies were presented—far too many to include in the brief time allotted for this presentation. I have selected a limited number of studies that emphasize the range of topics and innovative approaches covered in the neurosciences.

## Protein Aggregation Pathologies

In recent years studies on protein aggregation pathologies have made up a large proportion of the neuroscience studies submitted for consideration and presentation at this meeting. This year was no exception, with tau imaging studies joining amyloid imaging as an important focus.

Lao et al. from the New York State Institute for Basic Research in Developmental Disabilities (Albany, NY), the University of Pittsburgh Medical Center (PA), and the University of Wisconsin, Madison, presented “Longitudinal study of amyloid- $\beta$  accumulation in Down syndrome” [17], a condition that we know is prone to amyloid deposition. The researchers looked at a cohort of nondemented adults with Down syndrome who underwent  $^{11}\text{C}$ -Pittsburgh compound B ( $^{11}\text{C}$ -PiB) imaging at baseline and at  $\sim 3$ -year follow-up. Changes in amyloid deposition over time are summarized in Figure 1. Resulting images classified the participants into 3 groups: those who were amyloid-negative at baseline and remained negative, those who were amyloid-negative at baseline and converted to positive, and those who were amyloid-positive at baseline and whose amyloid load increased with time. The results indicated that a greater number of participants were actually amyloid-negative at baseline and that the conversion seemed to occur primarily in the striatal regions. This is interesting, because we know these regions are more susceptible to early amyloid tracer uptake in

familial Alzheimer disease (AD) than in typical age-associated sporadic AD. This study also raises the question of the best approach to measuring amyloid deposition over time, a crucial issue in developing both clinical trials and therapeutic approaches.

Another important study in this context came from Whittington et al. from Imanova Ltd. (London, UK) and Imperial College London (UK), who reported that “Spatiotemporal distribution of  $\beta$ -amyloid in AD results from heterogeneous regional carrying capacities” [346]. These researchers postulated that amyloid aggregation in different brain regions depends on the specific carrying capacities of the regions rather than the speed of amyloid growth. Drawing on data from the Alzheimer's Disease Neuroimaging Initiative, they calculated SUV ratios (SUVr) for cortical and subcortical regions from  $^{18}\text{F}$ -AV45 PET imaging in  $>700$  individuals with AD, early mild cognitive impairment (MCI), late MCI, and healthy controls. Their modeling approach allowed them to analyze differences in amyloid uptake in various regions of the brain (Fig. 2). They concluded that their results support the hypothesis that the process of regional accumulation of  $\beta$ -amyloid

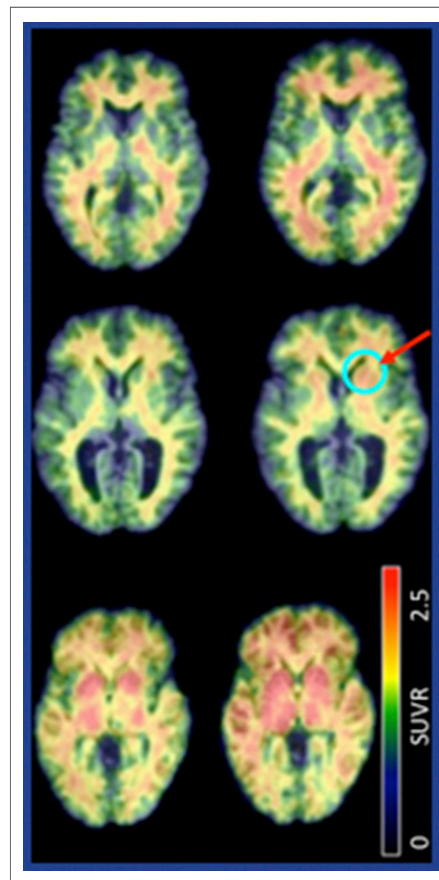


**FIGURE 1.** Quantification of amyloid deposition. Global  $^{11}\text{C}$ -PiB imaging in nondemented adults with Down syndrome identified 3 groups at baseline and 3-year follow-up who were: amyloid-negative at baseline and remained negative (top); amyloid-negative at baseline and converted to positive (middle); and amyloid-positive at baseline and with increasing amyloid load (bottom).

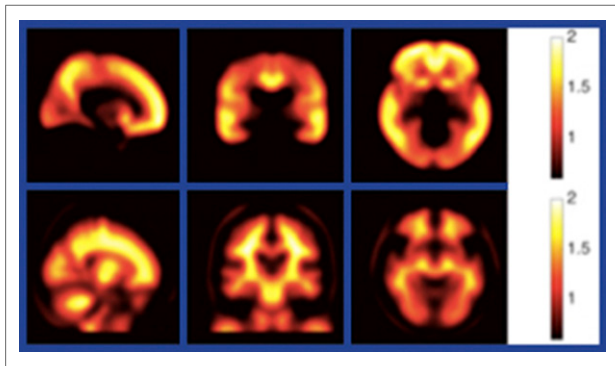


**FIGURE 2.** Modeling of SUV ratios for cortical and sub-cortical regions from  $^{18}\text{F}$ -AV45 PET imaging in individuals with cognitive impairment showed the importance of differences in regional carrying capacities (top) in development of amyloid accumulation compared with non-specific binding capacities (bottom).

“originates at the same time with the same growth rate for all regions, and it is the different regional carrying capacities that lead to the hierarchical distribution and not some longer time scale spreading phenomena from a limited number of seed regions.”

It is not clear why different brain regions would have different capacities for amyloid uptake, but one study presented at the meeting may provide clues. Minoshima et al. from the University of Utah (Salt Lake City) presented “Peak location of amyloid PET tracer uptake within cortical gray matter: topographic patterns and diagnostic application in AD” [512]. The authors examined the distance of the maximum amyloid peak in a perpendicular line from the brain

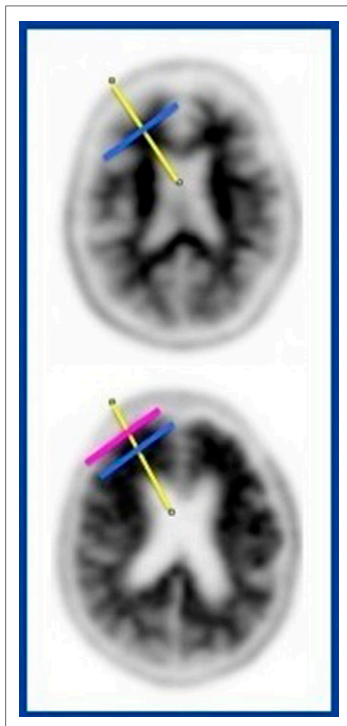


**FIGURE 3.** Peak location of  $^{18}\text{F}$ -florbetapir uptake on PET in amyloid-negative (top) and amyloid-positive (bottom) individuals. Yellow line = distance measured; blue line = gray matter/white matter interface; purple line = amyloid cortical laminar deposition.

center to the cortical border. In healthy subjects,  $^{18}\text{F}$ -florbetapir uptake is focused in white matter, whereas in amyloid-positive patients it extends into the gray/white matter interface. The distance between the peak gray matter uptake of amyloid tracer and the gray/white matter interface was assessed in 165 healthy controls and in 148 patients, with resulting values displayed on a surface projection in a normalized map (Fig. 3). Figure 4 shows the peak distance value in the AD group compared with that in the control group. These values look quite similar to the conventional analysis of SUVr-based analyses of maximum amyloid peak uptake in the brain. The authors were able to demonstrate that these peak distance analyses can differentiate healthy individuals from those with AD. This is important, because peak distance analysis does not require a reference region and is therefore not susceptible to the changes or variabilities in reference regions that are inherent with SUVr-based methods.

Villemagne et al. from Austin Health (Heidelberg and Melbourne, Australia), the Australian eHealth Research Center (Brisbane), and the University of Melbourne (Australia) presented “Generating continuous and categorical measures from tau imaging studies with  $^{18}\text{F}$ -AV1451 and  $^{18}\text{F}$ -THK5351” [128]. They developed a specific scale to evaluate uptake for  $^{18}\text{F}$ -AV1451,  $^{18}\text{F}$ -THK5351, and  $^{18}\text{F}$ -THK5317. The Tau MeTeR scale (mesial temporal, temporoparietal, and rest of the cortex) mirrors the steps of tau distribution across brain regions as identified by Broca and colleagues. They assessed the different tau tracers and found that, using these regions, it is possible to differentiate quite nicely between stages of disease and between healthy individuals and controls, as well as to define thresholds for each individual tracer. In addition, using this method they were able to demonstrate that tau uptake in the mesial temporal lobes in amyloid-positive and -negative healthy controls correlated with episodic memory, suggesting an age-related association. High tau uptake within the temporoparietal lobes in amyloid-positive MCI subjects correlated with impairments in episodic memory. High tau in the rest of the cortex in

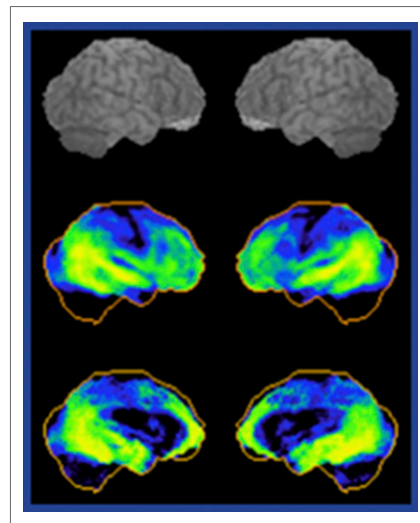


**FIGURE 4.** Deviation of peak distance of  $^{18}\text{F}$ -florbetapir uptake on PET in patients with Alzheimer disease and controls. Top: reference brain images. Bottom: Right (left) and left (right) lateral images derived from location-based algorithm using 3D surface projections of peak location of cortical laminar deposition.

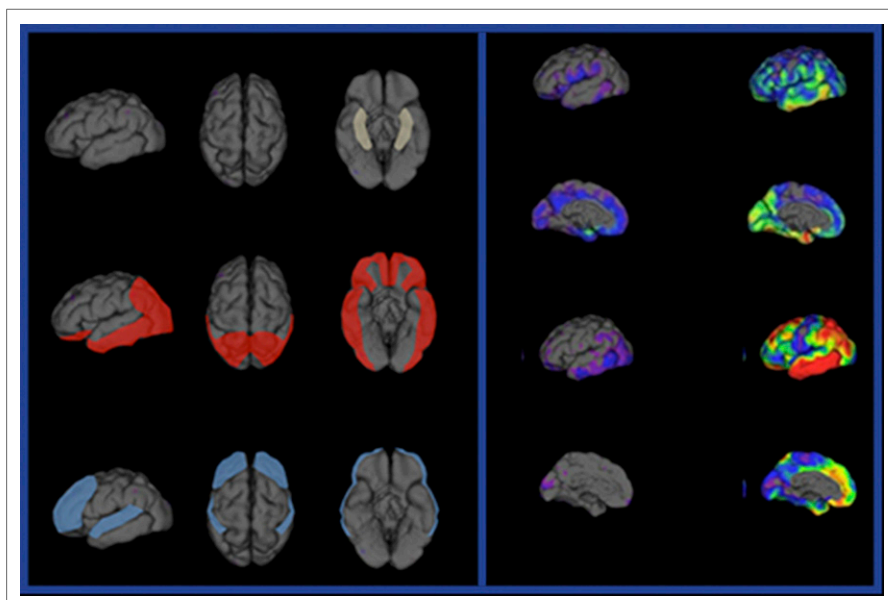


**FIGURE 5.** Left panel: Regional differences in tau distribution across brain regions as assessed by the Tau MeTeR scale. Left to right: left lateral, superior, inferior views. Top: Mesial temporal, high tau in amyloid-positive and -negative healthy controls correlating with episodic memory; middle: temporoparietal, high tau in amyloid-positive mild cognitive impairment (MCI) correlating with episodic memory; bottom: rest of cortex, high tau in amyloid-negative MCI correlating with non-memory decline. Right panel: Summed results in tau imaging of MCI with  $^{18}\text{F}$ -THK5351 (top 4 images) and  $^{18}\text{F}$ -AV1451 (bottom 4 images).

amyloid-negative individuals with MCI correlated with non-memory-associated cognitive decline, suggesting another form of disease in these subjects (Fig. 5).

Bischof et al. from the German Center for Neurodegenerative Diseases (Bonn), the Institute of Neuroscience and Medicine Research Center (Jülich, Germany), and University Hospital of Cologne (Germany) presented “Differential contributions of amyloid and tau burden to neurodegeneration in AD: a multimodal in vivo PET study” [124]. This group used 3 tracers in the brain:  $^{11}\text{C}$ -PiB to look at amyloid deposition,  $^{18}\text{F}$ -AV1451 to look at tau, and  $^{18}\text{F}$ -FDG PET to look at hypometabolism in 10 patients with AD (Fig. 6). The z-score values for the 3 tracers were extracted and compared. Results showed amyloid distribution to occur diffusely across the entire brain, whereas tau deposition was restricted to specific brain areas. These areas correspond topographically to regions of neuronal dysfunction measured by  $^{18}\text{F}$ -FDG PET (Fig. 7). The authors concluded that tau accumulation appears to impact neuronal function more directly than amyloid deposition in the brain. A direct correlation was found between tau deposition and hypometabolism, emphasizing the potential for tau pathology as a target for disease-modifying strategies in AD.

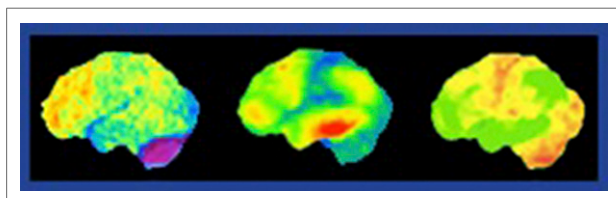


**FIGURE 6.** Multitracer PET imaging clearly characterized mild-to-moderate Alzheimer disease by assessing: amyloid deposition with  $^{11}\text{C}$ -PiB (left); tau fibrillary tangles with  $^{18}\text{F}$ -AV1451 (middle); and hypometabolism with  $^{18}\text{F}$ -FDG (right).

A similar study came from Iaccarino et al. from the Berkeley National Laboratory (CA), San Raffaele Scientific Institute (Milan, Italy), the University of California Berkeley (CA), and the University of California San Francisco, who presented “Evaluation of the associations between  $^{11}\text{C}$ -PiB and  $^{18}\text{F}$ -AV1451 PET retention and MRI atrophy in AD” [18]. Spatial distribution images (Fig. 8) in patients with probable AD and positive  $^{11}\text{C}$ -PiB PET suggest that amyloid is regionally diffuse, whereas tau and MR-detected atrophy appear to be more region-specific. Although no correlation was found between amyloid deposition and atrophy on a voxel-based assessment, associations were identified between tau and atrophy. Correlations between amyloid and tau were

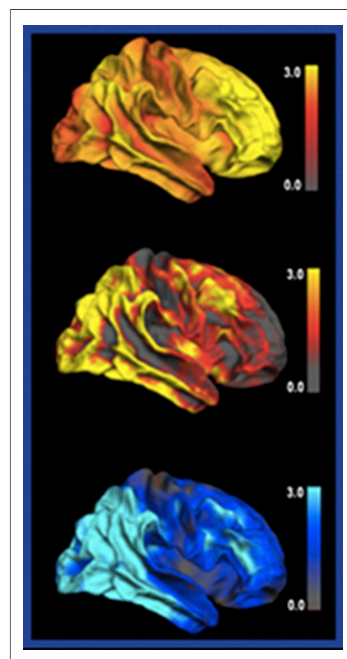


**FIGURE 7.** Topographical summed maps showing: amyloid plaques as assessed with  $^{11}\text{C}$ -PiB PET (top); tau fibrillary tangles as assessed by  $^{18}\text{F}$ -AV1451 PET (middle); and neuronal dysfunction as assessed by  $^{18}\text{F}$ -FDG PET (bottom). This figure was named as the SNMMI 2016 Image of the Year.

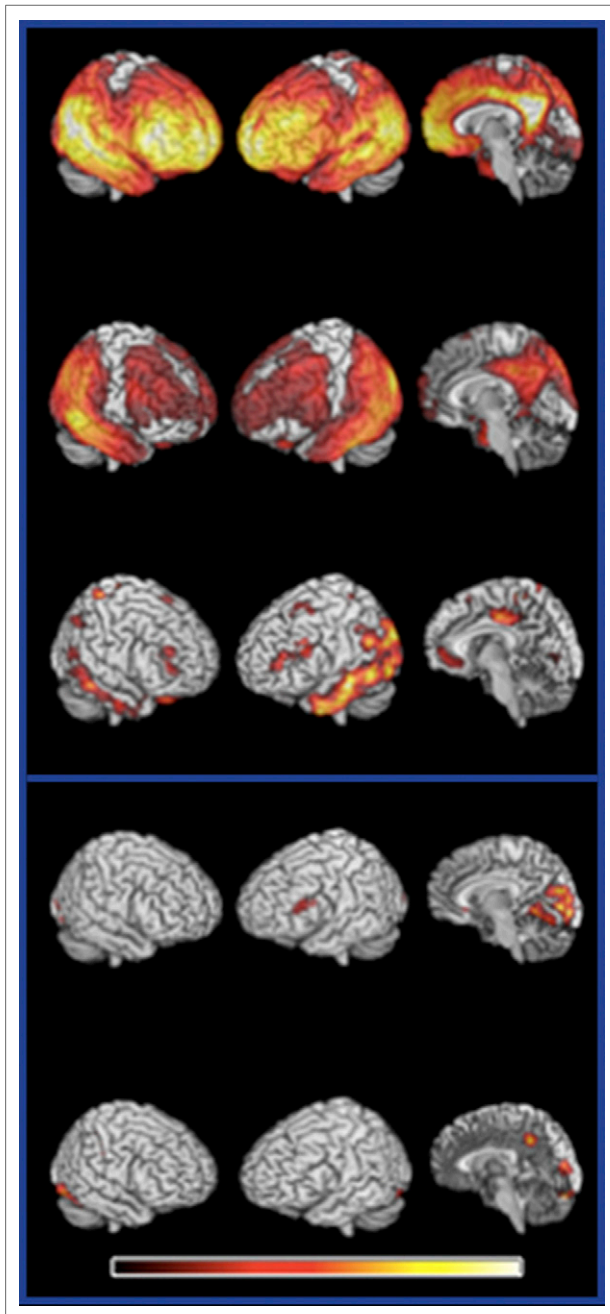


**FIGURE 8.** Top 3 rows: Spatial distributions of 2 PET tracers and MR-assessed atrophy as compared with data from healthy controls in individuals with probable Alzheimer disease. Top:  $^{11}\text{C}$ -PiB; middle:  $^{18}\text{F}$ -AV1451; bottom: atrophy. Bottom 2 rows: Biological parametric mapping voxel-wise robust regression modeling estimated correlations between PET tracers and atrophy. Top:  $^{18}\text{F}$ -AV1451 vs atrophy; bottom:  $^{11}\text{C}$ -PiB PET vs  $^{11}\text{C}$ -PiB PET. No correlation was found between  $^{11}\text{C}$ -PiB and atrophy.

also found, but only in selected regions. The lack of a larger correspondence with MR-assessed atrophy may be explained by the occurrence of such atrophy later in the disease course, a finding that fits well with our evolving concepts of AD progression.

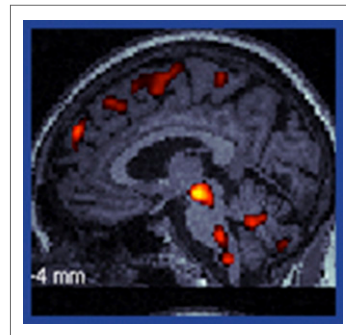


**FIGURE 9.**  $^{18}\text{F}$ -THK-5351 PET image acquired in a patient with clinically diagnosed progressive supranuclear palsy. Distinct tracer uptake in the midbrain correlated clearly with degree of disease.

### Movement Disorders

Vettermann et al. from the German Centre for Neurodegenerative Diseases (Munich, Germany), Tohoku University (Sendai, Japan), and the University of Munich (Germany) described the use of “ $^{18}\text{F}$ -THK-5351 PET in patients with clinically diagnosed progressive supranuclear palsy” [457]. Supranuclear palsy is characterized by tauopathy. Six patients with probable supranuclear palsy underwent  $^{18}\text{F}$ -THK-5351 PET imaging, with results showing distinct tracer uptake in the midbrain correlating clearly with degree of disease (Fig. 9). The researchers concluded that tau imaging might be a useful biomarker for tau deposition and might facilitate earlier and more reliable diagnosis of progressive supranuclear palsy.

Seibyl et al. from the Institute for Neurodegenerative Disorders (New Haven, CT) presented “Regional striatal differences in the rate of dopamine transporter loss in the Parkinson Progression Marker Initiative: relevance to clinical trial design” [70]. They analyzed data from a multicenter study using  $^{123}\text{I}$ -ioflupane SPECT to measure dopamine transporter (DAT) density in a group of de novo clinically classified volunteers with Parkinson disease (PD) over a period of 4 years or more. In bilateral and regional analyses of the striatum they found an average 10%–12% decrease in DAT density in the first 2 years, but this decline slowed to

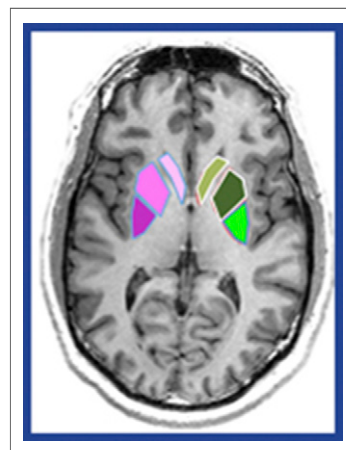


**FIGURE 10.** Summed results of serial  $^{123}\text{I}$ -ioflupane SPECT images acquired at baseline and at 2-year follow-up in patients with newly diagnosed Parkinson disease showed regional striatal differences in rates of dopamine transporter (DAT) loss. In the less affected hemisphere, DAT density decreases were observed in the posterior putamen (dark purple), less marked in the anterior putamen (medium purple), and even less marked in the caudate nucleus (light purple).

This well-delineated order of DAT density decrease was not observed in corresponding areas (green) of the more affected hemisphere.

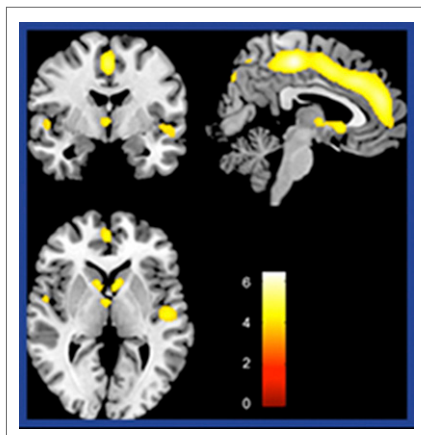


**FIGURE 11.**  $^{18}\text{F}$ -FPEB PET and decreased limbic metabotropic glutamate receptor subtype 5 availability in alcohol dependence. Results comparing imaging in individuals with alcohol dependence and healthy controls indicated a significant role of the glutamatergic system in addiction.

$\leq 7\%$  in later years. Rates of decline were highly region-specific. Most interesting, in areas of the less affected hemisphere, they found a clear rank order of decrease, with the highest decrease in the posterior putamen, less marked decrease in the anterior putamen, and even less marked decrease in the caudate nucleus. This well-delineated order of DAT density decrease was not observed in the more affected hemisphere in the brain, where declines seemed to be more equal across the regions (Fig. 10). The authors concluded that these observations are related to the variability seen in early stages of PD and that areas with greatest signal change and lowest variability (such as the caudate) might be more sensitive for detecting slowing rates of change with disease-modifying therapies.

#### Receptor Imaging in Psychiatry and Psychiatric-Associated Disorders

Leurquin-Sterk et al. from the University of Leuven (Belgium), University Hospital Gasthuisberg (Leuven, Belgium), and the University of Antwerp (Belgium) reported that “Alcohol addiction is associated with decreased limbic metabotropic glutamate receptor subtype 5 (mGluR5) availability: a  $^{18}\text{F}$ -FPEB PET study in humans” [15]. Sixteen recently abstinent alcohol-dependent individuals underwent imaging, with measurement of mGluR5 availability. Results showed decreases in regional availability in the limbic system (Fig. 11). These were quite significant changes, which also correlated with levels of alcohol consumption in the weeks and months preceding imaging. However, the researchers also identified an area of the insular cortex with higher glutamate receptor availability, directly corresponding to higher craving. The authors concluded that clearly the glutamatergic system is playing a major functional role in the pathophysiology of alcohol addiction, an observation that corresponds to recent clinical PET findings on nicotine and cocaine addiction.

Worhunsy et al. from the University of New Mexico (Albuquerque) and the Yale University School of Medicine (New Haven, CT) presented “Concurrently upregulated and downregulated  $\text{D}_2/\text{D}_3$  receptor systems in cocaine use disorder using  $^{11}\text{C}$ -PHNO” [16]. Twenty-six recently abstinent

individuals with cocaine use disorder and 26 healthy controls underwent PET imaging, and  $\text{D}_2/\text{D}_3$  receptor availability was measured using a complex independent component analysis (ICA). Results identified 2 important and different changes in the dopaminergic system in addicted individuals: downregulation of binding potential in the striatopallidal region (Fig. 12, green) and upregulation in the pallidonigral region (Fig. 12, blue). Most interesting was the fact that the 2 could overlap, as I have tried to illustrate by creating a fusion image. If  $\text{D}_2/\text{D}_3$  receptor availability had been measured in this region using a region-of-interest-based analysis, the differences in regional binding potential would not have been detected because the 2 receptor types are available and overlapping. The ICA approach identifies these differences even in overlapping receptor regions, making it a very intelligent method for analysis of receptor imaging data.

Wooten et al. from the Harvard Medical School/Massachusetts General Hospital (Boston, MA) reported on “Inhibitory and excitatory responses of the serotonin system: a simultaneous PET/fMRI study” [351]. They performed multiple serial  $^{11}\text{C}$ -MDL100907 PET/iron oxide contrast-enhanced functional MR studies in rhesus macaques to examine the excitatory effects of the  $5\text{-HT}_{2\text{A}}$  receptor subtype and the inhibitory effects of the  $5\text{-HT}_{1\text{A}}$  receptor subtype using subtype-specific agonist and antagonist drugs. This was an extraordinarily complex study, the results of which

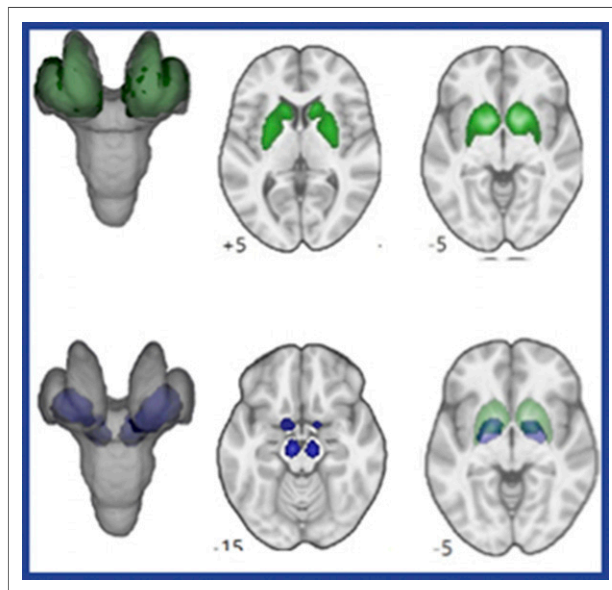


**FIGURE 12.** Independent component analysis was used to extract independent sources of  $[^{11}\text{C}]\text{PHNO } BP_{\text{ND}}$  from parametric volumes across subjects. Top: The striatopallidal source (green) was associated with regional  $\text{D}_2$ -related binding potential of a lower intensity in cocaine use disorder (CUD) participants and negatively correlated with years of cocaine use. Bottom: The pallidonigral source (blue) was associated with regional  $\text{D}_3$ -related binding potential, of a greater intensity in CUD participants and positively correlated with years of cocaine use. Overlap between the up- and downregulated areas can be seen in the fused image (bottom right).

I have simplified in Figure 13, using the analogy of a water faucet, with the excitatory system on the hot water side and the inhibitory system on the cold water side. In those instances where PET showed low endogenous serotonin levels, the application of an agonist of the excitatory system would result in activation of the brain, as expected. Application of an agonist of the inhibitory system would result in a decrease in brain activation. Application of antagonists would not have a major effect, because (continuing with the faucet analogy) if the faucets are already almost entirely closed and are then closed further, the

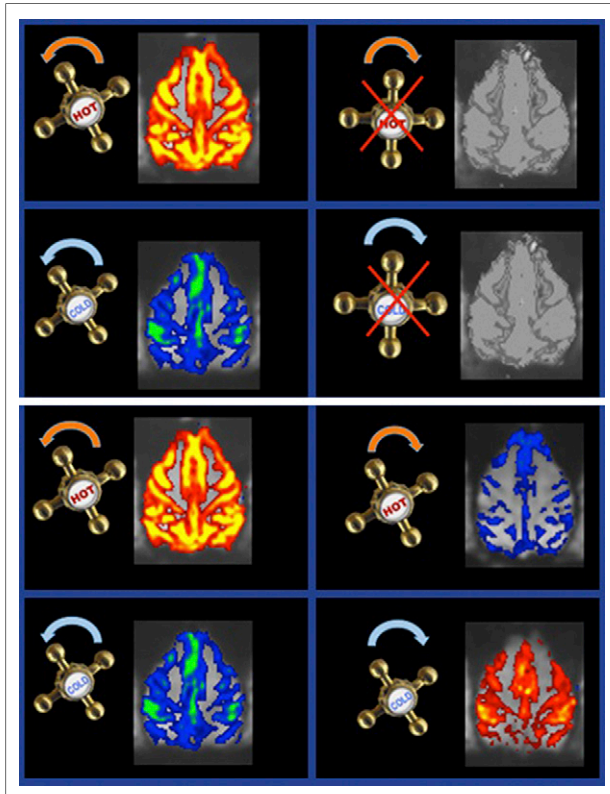


**FIGURE 13.**  $^{11}\text{C}$ -MDL100907 PET/functional MR imaging of inhibitory and excitatory responses of the serotonin system in rhesus macaques. The principle of these studies is illustrated using an analogy of a faucet, with the excitatory system on the hot water side and the inhibitory system on the cold water side. **Top block:** Under baseline conditions, serotonin levels are low (i.e., the faucet is closed). Left: Activation of the excitatory 2A system with a 5-HT<sub>2A</sub> agonist would lead to brain activation (like opening the hot water tap, top). Activation of the inhibitory 1A system with a 5-HT<sub>1A</sub> agonist would lead to deactivation (like opening the cold water tap, bottom). Right: Application of antagonists would not have a major effect, because (continuing with the faucet analogy) if the faucets are already almost entirely closed and are then closed further, the entire system will not be affected. **Bottom block:** The situation is different when PET identifies high endogenous serotonin levels, in which case the metaphorical faucet is open and running. In this situation, the application of a 5-HT<sub>2A</sub> antagonist “turns down” the hot water, with a decrease in activation. If a 5-HT<sub>1A</sub> antagonist is applied to the inhibitory system (turning down the cold water), the result will be an increase in brain activation.

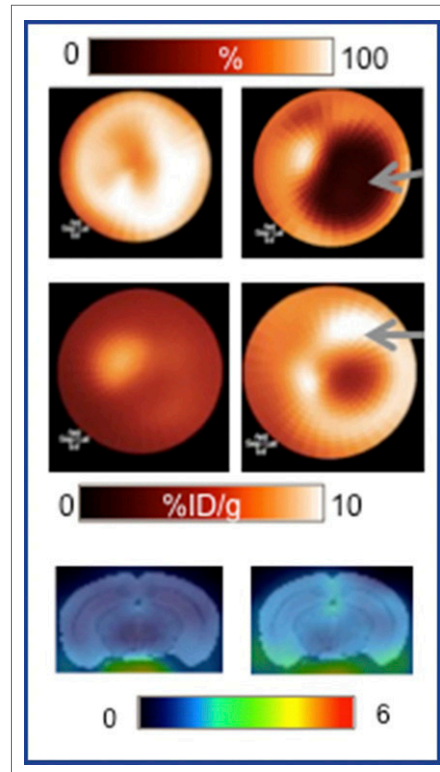


**FIGURE 14.** Systemic analysis of neuroinflammation after myocardial infarction (MI) using translocator protein (TSPO)-targeted molecular imaging. Images acquired in a sham-operated mouse (left) and in a mouse 3 days after coronary occlusion (right). Top block: SPECT (top) shows area of infarction (arrow).  $^{18}\text{F}$ -GE180 PET (middle block) shows area of inflammation (arrow). Bottom block: Concurrent brain images demonstrated parallel increases in brain TSPO

signal, suggesting systemic inflammation in response to MI. Later-stage increases in TSPO in the brain and heart paralleled declining cardiac function, suggesting a link to progressive heart failure.

entire system will not be affected. However, the situation is different when PET identifies high endogenous serotonin levels, in which case the metaphorical faucet is open and running. In this situation, the application of an antagonist “turns down” the hot water, with a decrease in activation. If an antagonist is applied to the inhibitory system (turning down the cold water), the result will be an increase in brain activation. The authors concluded that their findings “support the validity of a functional MRI construct sensitive to receptor-mediated signaling and pave the way toward joint PET/fMRI modeling of pharmacological action in the serotonergic system.” This study very nicely demonstrates a way in which multimodal imaging may allow us to explain complex systems in the brain that cannot in any other way be assessed.

### Inflammation

Inflammation is increasingly recognized as an important factor influencing different forms of brain disorder, ranging from depression to neurodegeneration. Hupe et al. from the Hannover Medical School (Germany) reported that “Myocardial infarction is associated with neuroinflammation—a systemic analysis using translocator protein (TSPO)-targeted molecular imaging” [404]. In a mouse model of coronary occlusion, they used electrocardiograph-gated myocardial

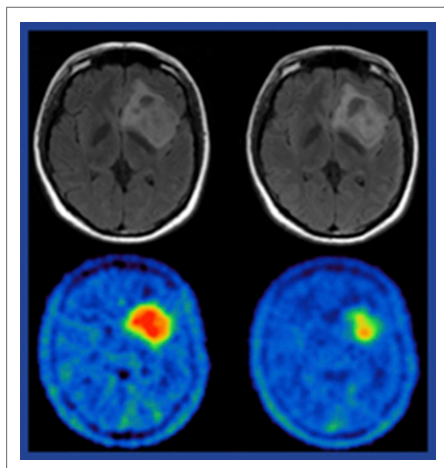


**FIGURE 15.**  $^{18}\text{F}$ -FET PET for chemotherapy monitoring in non-contrast-enhancing gliomas. Top: MR T2-FLAIR imaging before temozolomide chemotherapy (left) and 6 months after (right) indicated stable disease. Bottom: Biologic tumor volume and maximum tumor-to-background ratio derived from  $^{18}\text{F}$ -FET PET imaging at the same timepoints as MR indicated a >25% reduction in amino acid uptake.

perfusion SPECT to measure inflammation and  $^{18}\text{F}$ -GE180 PET to assess TSPO. As expected, a rim of inflammation was identified around the area of infarction, but the researchers also looked at the brain, where they found an increase in inflammatory signal directly corresponding to the increase in inflammatory signal in the heart (Fig. 14). When the experimental animals were re-imaged over time, fluctuations in the cardiac inflammatory signal were exactly mirrored in the brain, suggesting that the inflammatory response to ischemia in the heart is a systemic effect rather than a regionally localized effect. This is a nice study, bridging the cardiac and neurologic applications of multimodal tracer imaging.

### Brain Tumors

Unterrainer et al. from Ludwig-Maximilians-Universität Munich (Germany) reported on the “Value of  $^{18}\text{F}$ -FET PET for chemotherapy monitoring in non-contrast-enhancing gliomas” [14]. Their aim was to monitor treatment response. A significant portion of gliomas do not show contrast enhancement. This study included 61 patients with histologically proven grade 2–3 gliomas who underwent MR and PET imaging before and 6 months after initiation of temozolomide or procarbazine/lomustine/vincristine chemotherapy. The results clearly indicated that patients who showed a decrease in amino acid uptake under therapy had the best overall survival rate at 6 months (Fig. 15). Patients whose amino acid uptake was stable over the same period had relatively good survival, whereas those who showed increases, likely reflecting continued tumor growth, had the lowest survival rates. This study, then, demonstrates the clinical value of  $^{18}\text{F}$ -FET PET imaging in a specific population. The authors also concluded that this high association between  $^{18}\text{F}$ -FET PET results and survival suggests that, “in contrast to MRI,  $^{18}\text{F}$ -FET PET can therefore identify treatment responders and nonresponders at an early stage and might help to improve patient management.”

Kobayashi et al. from the Hokkaido University Graduate School of Medicine (Sapporo, Japan) reported that “Texture analysis of  $^{11}\text{C}$ -methionine PET may help glioma grading” [179]. Texture analysis has become a buzzword, frequently used in radiology studies. The basic concept is that the computer can see things that the human eye does not, by identifying specific and recurring patterns in the structures of imaging information. These authors applied texture analysis in  $^{18}\text{F}$ -MET PET/CT images acquired in 46 patients with brain tumors. Two of the results were quite interesting. One was that low-grade gliomas could be distinguished from high-grade gliomas using the texture features (Fig. 16). In the case illustrated, I should note, the difference between the low- and high-grade cases is visually apparent. However, the group also documented the ability of texture analysis to identify an oligodendroglial component in a glioma, something that is not visually evident. The authors noted that the ability of texture analysis to detect and potentially grade oligodendroglial components in gliomas may have potential in prognosis and management. This study has a broader significance: I believe that we should explore these modern data analysis methods more vigorously in our field, because molecular imaging data has the potential to contain more “hidden” information than structural imaging, in which these methods are currently more frequently used.

### Summary

One major trend in the neuroscience presentations at this year’s SNMMI meeting was the growing application of computer programs and data analysis to brain imaging data. In an increasing number of studies, observer-independent or computer-supported approaches were applied to data

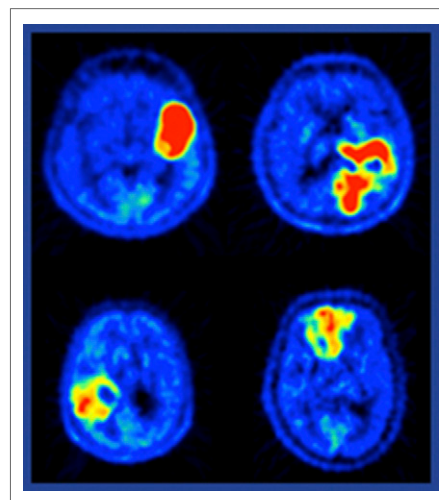


**FIGURE 16.** Texture analysis of  $^{11}\text{C}$ -methionine PET in glioma grading. Top: Representative images of grade III (left) and 4 (right) gliomas. Conventional  $\text{SUV}_{\text{max}}$  and tumor-to-normal tissue ratios were similar, but the long-zone high gray-level emphasis texture value was higher in grade 3 than grade 4. The

grade 4 glioma has a visually identifiable distorted shape and nonuniform distribution. Bottom: Representative images of grade 4 glioblastomas without (left) and with (right) an oligodendroglial component. The lesion with an oligodendroglial component has a lower short-zone low grey-level emphasis texture value than the lesion without oligodendroglia, with little or no visually discernible difference.

evaluation. I believe that this suggests that artificial intelligence will soon enter the imaging arena in nuclear medicine, an eventuality for which we should be preparing now. A second major trend was seen in multimodal studies in both humans and animals to investigate physiologic and pathophysiologic interactions in the brain.

To conclude, I would like to cite Henry N. Wagner, Jr., MD, who, in turn, once quoted Arthur Koestler: “In biology,

structures are slow processes of long duration; what we call functions are fast processes of short duration.” Dr. Wagner added that they are all processes—changes in mass as a function of time. This observation leads to the conclusion that the methods we have available in our field for functional, structural, and molecular imaging allow us nothing less than the ability to assess biological processes of different speed and duration *in vivo*.

## SNMMI Wagner–Torizuka Fellowships Announced

**S**NMMI announced on August 23 the recipients of the 2016–2018 SNMMI Wagner–Torizuka Fellowships. This 2-year fellowship, founded in 2008 by Henry N. Wagner, Jr., MD, and Kanji Torizuka, MD, PhD, is designed to provide training and experience in nuclear medicine and molecular imaging for Japanese physicians in the early stages of their careers. “SNMMI is proud to sponsor the Wagner–Torizuka Fellowship. Each year, the program provides 3 outstanding Japanese scientists in the field of nuclear medicine and molecular imaging with 2 years of funding to further their research in the United States under the guidance of current leaders in the field,” said Gary L. Dillehay, MD, SNMMI past president and 2014–2016 chair of the SNMMI Awards Committee. The 2016–2018 fellows, who will receive annual stipends of \$24,000, are:

- **Kimiteru Ito, MD, PhD**, Tokyo Metropolitan Geriatric Hospital and Institute of Gerontology (Tokyo, Japan), whose research focuses on associations between the therapeutic efficacy of checkpoint inhibitors and  $^{18}\text{F}$ -FDG PET/CT findings, as well as interim  $^{18}\text{F}$ -FDG PET/CT and prognosis in patients with T-cell lymphoma. Ito is currently a visiting researcher in the molecular imaging and therapy service at the Memorial Sloan–Kettering Cancer Center (New York, NY) under the supervision of Wolfgang Weber, MD.

- **Akira Toriihara, MD, PhD**, Tokyo Medical and Dental University (Japan), whose research interests include development of semiquantitative assessments of SPECT/CT using  $^{67}\text{Ga}$ -citrate and  $^{123}\text{I}$ -ioflupane. Toriihara is studying at Stanford University School of Medicine (CA) in the Department of Radiology’s Nuclear Medicine and Molecular Imaging Division under the supervision of Andrei Iagaru, MD.
- **Takuya Toyonaga, MD**, Hokkaido University Graduate School of Medicine (Sapporo, Japan), who is researching  $^{11}\text{C}$ -UCB-J as a radioligand for imaging synaptic vesicle glycoprotein 2A and its potential application in Alzheimer disease. Toyonaga is studying at the Yale School of Medicine PET Center (New Haven, CT) under the supervision of Richard Carson, PhD.

The SNMMI Wagner–Torizuka Fellowship program, sponsored by Nihon Medi-Physics Co., Ltd., in Japan, has successfully graduated 24 fellows since its inauguration in 2008. Five fellows are currently studying at host institutions across the United States. Applications and additional information about requirements for the 2017–2019 SNMMI Wagner–Torizuka Fellowship are available online at [www.snmmi.org/grants](http://www.snmmi.org/grants). Applications are due by January 20, 2017. For more information about these and other scholarships, visit [www.snmmi.org/grants](http://www.snmmi.org/grants) or contact the SNMMI Development Department at 703-652-6780 or at [tellmer@snmmi.org](mailto:tellmer@snmmi.org).